Article

Simulation of Biogas Upgrading by Sorption-Enhanced Methanation with CaO in a Dual Interconnected Fluidized Bed System

Fiorella Massa [1], Fabrizio Scala [1,2,*] and Antonio Coppola [1]

[1] Istituto di Scienze e Tecnologie per l'Energia e la Mobilità Sostenibili, Consiglio Nazionale delle Ricerche, Piazzale V. Tecchio 80, 80125 Napoli, Italy; fiorella.massa@stems.cnr.it (F.M.); antonio.coppola@stems.cnr.it (A.C.)

[2] Dipartimento di Ingegneria Chimica, dei Materiali e della Produzione Industriale, Università degli Studi di Napoli Federico II, Piazzale V. Tecchio 80, 80125 Napoli, Italy

[*] Correspondence: fabrizio.scala@unina.it

Abstract: In this work, ASPENplus was used to simulate biogas upgrading by sorption-enhanced methanation in a dual interconnected bubbling fluidized bed configuration using inexpensive, abundant, and eco-friendly CaO to remove H_2O from the reaction environment. The chemical looping scheme consisted of two reactors: a methanator/hydrator, where the catalytic reactions occurred on a catalyst with 20% Ni supported on alumina as well as the steam removal by CaO, and a regenerator, where the $Ca(OH)_2$ was dehydrated back to CaO. The simulations were carried out to identify possible reactant compositions (H_2 and biogas), CaO amount, and the methanation temperature able to produce an outlet gas matching the specifications for direct grid injection. When considering a stoichiometric gas feed ratio at the methanator inlet, the unwanted CaO carbonation worsened the process performance, subtracting CO_2 from the desired methanation reaction. However, optimal conditions were found with hydrogen-lean gas feedings, balancing the limited H_2 amount with the capture of CO_2 due to the sorbent carbonation. Thermodynamic considerations pointed out the possibility of solid carbon formation induced by sorption-enhanced methanation conditions, especially for H_2 sub-stoichiometric feedings.

Keywords: sorption enhanced methanation; biogas upgrading; Aspen simulation; calcium oxide; sorbent hydration; dual interconnected fluidized beds

1. Introduction

In the framework of the efforts to address the energy transition, a renewed attention is growing for the catalytic or biological processes to produce synthetic renewable methane (synthetic or substitute natural gas—SNG). This is due to the crucial role played in numerous sectors by this important energy carrier, which benefits from a developed storage and distribution infrastructure in many countries, and a large public acceptance. Catalytic paths to renewable methane production can involve either valorization of residual biomass by gasification and subsequent syngas methanation, or CO_2 methanation combined with power-to-gas applications, converting surplus renewable electric energy into a grid-compatible gaseous fuel. This latter application includes using green hydrogen obtained by water electrolysis, either for methanation of CO_2 from streams of captured CO_2 (carbon capture and utilization—CCU), or for biogas upgrading to increase the methane content of streams from digestion of organic feedstock [1–3]. Referring to this last solution, biogas, its production has received attention as a promising renewable path for energy valorization of residual biomass, and it mostly consists of CH_4 (generally ca. 50–75%) and CO_2 (ca. 25–45%), with percentages determined by feedstock and digestion operating conditions. The most used feedstocks are sewage, farming residues, and the organic fraction of

domestic and industrial waste. The heterogeneity of these sources, besides the consequent technological challenges, also implies that the removal of contaminants in the gas phase is a sensitive issue, and there appears to be ample room for research, especially on the development of cost-effective materials [4]. Among the mentioned technological issues of anaerobic digestion, there are challenges such as the methods to reduce the inhibition of anaerobic sludge digestion by emerging contaminants, especially pharmaceuticals, for example. These rising matters have been recently addressed in the literature [5].

Although even trace amounts of species like H_2O, O_2, NH_3, and N_2 may need to be removed, the core upgrading stage for injection into the natural gas grid or usage as a fuel is CO_2 removal, with the separated CO_2 generally being released into the atmosphere. Conventional and well-established separation processes rely on absorption, adsorption, membrane, cryogenic, or biological removal [6]. An interesting alternative to such separation processes may be the further methanation of CO_2 in raw biogas to produce additional CH_4.

Catalytic CH_4 production, in addition to CO_2 hydrogenation (1), can occur via CO hydrogenation (2), according to the reactions discovered by Sabatier and Senderens in 1902 [7], with high exothermicity and a net decrease in moles:

$$CO_2 + 4H_2 \rightleftharpoons CH_4 + 2H_2O - 164 \text{ kJ/mol (@298K)}, \qquad (1)$$

$$CO + 3H_2 \rightleftharpoons CH_4 + H_2O - 206 \text{ kJ/mol (@298K)}. \qquad (2)$$
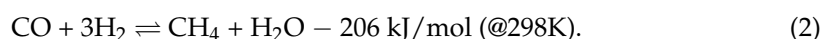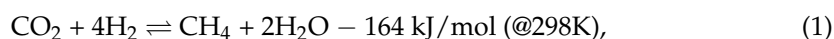
Commercial processes are generally found in ammonia synthesis plants to eliminate carbon monoxide traces and rely, due to the high exothermicity of the reactions, on a series of adiabatic catalytic fixed beds operated at temperatures between 250 and 600 °C with intermediate cooling steps and recycles, and at high operational pressure. Apart from the above-mentioned original industrial application, studies of synthetic natural gas (SNG) production as a standalone process have led to other commercial solutions being developed over the past decades. In the 1970s and 1980s, Haldor Topsøe carried out a steam reforming of methane using nuclear energy and then transported the synthesized gas to a heat-consuming site to be reconverted in a cyclic process by means of methanation, exploiting the high reaction enthalpy; TREMP stands for Topsøe's Recycle Energy efficient Methanation Process. The scheme consists of three adiabatic fixed bed reactors with a recycle to the first reactor, temperatures from 250 to 700 °C, pressure up to 30 bar, and a near-stoichiometric hydrogen to carbon oxides ratio at the inlet. The original project was completed but the TREMP process is still used to produce SNG from synthesis gas. The process has been demonstrated in plants of a semi-commercial scale, producing between 200 and 2000 Nm^3/h of SNG under realistic industrial conditions, and mainly relies on the purposely developed Topsøe MCR methanation catalysts which present high and stable activity in a wide temperature range [8]. On the other hand, the promising power-to-gas solution has been applied on an industrial scale in Audi motor company's "e-gas" facility in Werlte, Germany, where 1000 metric tons/year of synthetic natural gas (SNG) are produced using concentrated CO_2 from a nearby biogas plant [9].

The difficult temperature control appears to be a sensitive issue related to, for example, catalysts' stability and their deactivation in the presence of high temperature hotspots. Regarding methanation catalysts, if considering the main active phases (Ru, Ni, Fe, Co, and Mo), nickel is in general found in industrial solutions since it is quite inexpensive despite being significantly active and selective [2]. Unfortunately, in addition to thermal deactivation, commercial nickel catalysts are also subject to mechanical and chemical deactivation [10]. The latter is mainly represented by carbon generation and accumulation on the catalyst surface [11]. Because of the more efficient control of large-scale exothermic processes, fluidized beds have been suggested as a possible alternative to the consolidated fixed bed configurations [2].

Recently, among different research activities directed to innovate the traditional process, the sorption-enhanced methanation (SEM) concept has been proposed, based on Le

Chatelier's principle, to improve reaction performance by selectively removing produced steam from the reaction environment [12,13]. The local H_2O adsorption, by shifting the equilibrium toward the products generation, would allow for overcoming of thermodynamic constraints, improving methanation performance at relatively low pressure. This solution may be applied to reduce the energy duty for gas compression work. Early studies proposed sorption-enhanced CO_2 methanation [12] at atmospheric pressure and low temperatures (250 °C) and investigated nickel as an active metal and zeolite 4A as a sorbent in a cyclic series of regenerative experiments. Although an almost-unitary conversion was detected, the authors highlighted a worsening in terms of water capture (15–20%) due to the parallel CO_2 adsorption. These studies were first carried out by Walspurger et al. [12], focusing on biogas upgrading. They analyzed the thermodynamics of CO_2 methanation in ASPEN Plus under typical conditions found in industrial processes (CO_2 captured and hydrogen produced by electrolysis available at nearly 1 bar and 40 °C). The target was to obtain an SNG quality suitable for a certain gas grid of specifications at a pressure of 60 bar. The target of an injectable stream will also be considered in our study, considering average standards in the EU on a dry molar basis: $H_2 < 2\%$, $CO_2 < 2.5\%$, $CO < 0.5\%$. Walspurger et al. selected the traditional fixed bed configuration and modelled the influence of in situ water removal, considering the third reactor either as a conventional reactor or as a sorption-enhanced reactor. It was seen from the simulation that a water-removing reactor in place of the third conventional reactor led to a significantly lower H_2 level in the SNG and that the gas grid specifications could be matched at much lower operational pressure (nearly 30 bar compared to 60 bar of a conventional case). The authors pointed out that operating the methanation at relatively low pressure may determine a significant compression energy saving: more than 60% at pressures lower than 5 bar. The temperature increase aspect was also investigated by these authors, providing results that support the suggested application of fluidized bed reactors. In fact, at pressures below 10 bar the amount of CO_2 and H_2 to be converted in a sorption-enhanced reactor would lead to an excessive temperature rise, considering this process as a third step in a fixed bed reactor scheme.

Borgschulte et al. [13] demonstrated the enhancement using bifunctional materials combining sorption and catalyst properties by impregnating Ni on a zeolite 5A. Delmelle et al. [14] identified zeolite 13X as the sorbent with the highest steam adsorption capacity as a bifunctional material by adding Ni to its structure. Therefore, the key to the success of SEM technology relies on identifying a proper material to adsorb H_2O at the temperatures of interest for methanation, which are significantly high for an adsorption process, and to allow for its dehydration at temperatures that, although higher than the adsorption ones, could be acceptable in terms of catalyst operation and energy requirements. Generally, most of the studies in the literature involve fixed bed operation conditions. So far, chemical looping configurations with sorption-enhanced applications have involved mostly CO_2 removal in the sorption-enhanced steam reforming of ethanol [15–17].

By taking advantage of the favorable features of fluidized beds, SEM chemical looping based on the technology of coupled fluidized reactors would allow for steady operation [1], enabling continuous sorbent transfer and regeneration (Figure 1). In fact, despite the compact design of fixed beds configurations, these reactors would imply discontinuous SEM process, and difficult heat control on a large scale [2]. Coppola et al. [18] selected calcium oxide and a commercial zeolite 3A as sorbents, studying adsorption/desorption capacity over cycles in a chemical looping dual fluidized bed system. Zeolites, the most investigated sorbent in the literature, present a stable trend over the cycles; however, CO_2 competes with H_2O during the sorption process. CaO shows a decline in steam capture capacity under cyclic operation, induced also by the undesired carbonation reaction. CaO was also tested by Agirre and coworkers [19]; this sorbent seems to be promising for SEM application, even if possible negative effects on the catalyst call for additional studies. Despite several drawbacks, CaO is an appealing possibility because it is inexpensive, abundant, and ecofriendly, unlike zeolites.
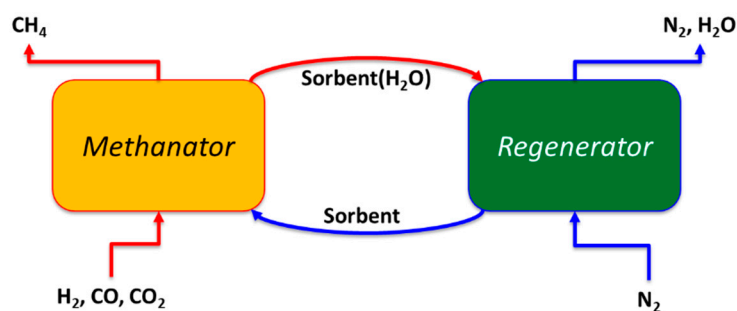
Figure 1. SEM concept scheme. Sorbent(H_2O) indicates the sorbent with adsorbed H_2O.

Sorption-enhanced methanation using CaO to perform biogas upgrading in a dual interconnected fluidized bed (DIFB) configuration was modelled in ASPENplus with the idea of detecting working conditions for the process in terms of feeding gas and CaO amounts, as well as methanation temperatures, to obtain product compositions suitable for direct injection in the natural gas grid. The results were also subjected to thermodynamic considerations in terms of possible coke deposition enhanced by SEM conditions. In fact, although carbon deposition during the traditional process occurs exclusively during CO methanation [6,20–23], thermodynamic studies demonstrated that SEM conditions may also enhance carbon formation during CO_2 methanation [24]. In particular, Catarina Faria et al. [6] analyzed the thermodynamics of CO_2 methanation under SEM conditions applied to a biogas upgrading process, pointing out the increased importance of carbon-generating reactions with a much more extensive carbon formation than in the absence of H_2O removal.

2. Materials and Methods

2.1. SEM Modelling

2.1.1. Aspen Flowsheet

ASPENplus V10 software was used to simulate the SEM process in a chemical looping DIFB configuration. The 'Fluidbed' blocks, as isothermal and one-dimensional reactors, were used, and the kinetics of all the main reactions was implemented in them. The flowsheet of the plant, operated at atmospheric pressure, is shown in Figure 2, where 'METH' and 'REGEN' indicate the methanator and the regenerator, respectively. For the 'METH' block, the methanation temperature was varied in a certain range (250–300–350 °C), while the 'REGEN' temperature was fixed at 450 °C; both reactors were simulated at nearly atmospheric pressure.
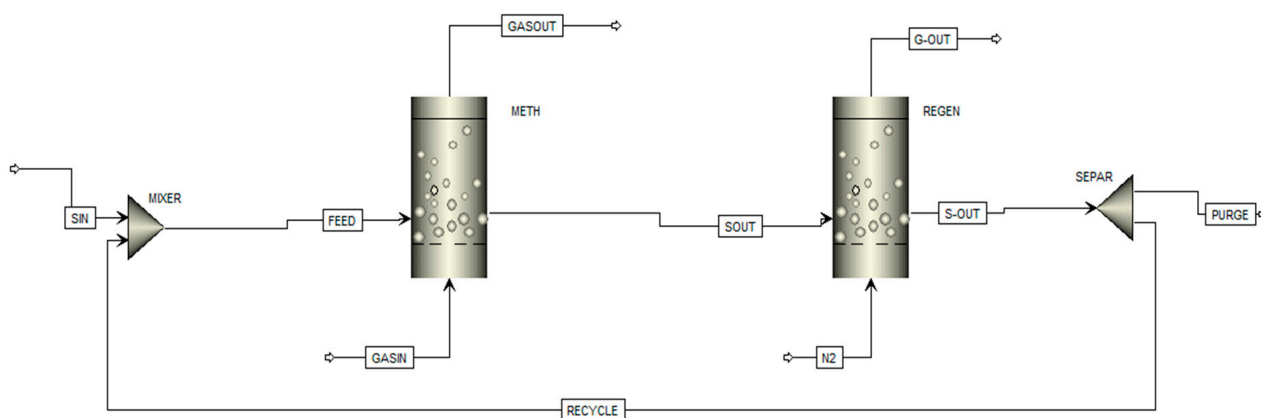
Figure 2. SEM process Aspen flowsheet.

Table 1 summarizes several parameters implemented for the SEM DIFB. The diameter of the methanator was varied to set a fluidization velocity equal to 1 m/s for the differ-

ent inlet biogas feeding conditions (with a fixed biogas inlet of 0.4 kmol/h) at the three methanation temperatures considered.

Table 1. Main parameters for the reactors.

Parameters	Methanator (METH)	Regenerator (REGEN)
Height, m	14	8
Internal diameter, m	0.099–0.147	0.33
Solid discharge height, m	1.4	0.64
Voiadge at u_{mf} [1], -	0.5	0.5
Geldart classification, -	B	B

[1] u_{mf} = minimum fluidization velocity.

The default or selectable correlations used in Aspen for modeling the bottom and freeboard zones, and particle size distribution (PSD); calculating the transport disengaging height (TDH); and determining the minimum fluidization velocity and the elutriation, are those found in the literature [25–28].

2.1.2. Kinetics

Table 2 reports the kinetics implemented for the simulations. In addition to the reactions previously introduced as (1) and (2), and the water-gas shift reaction kinetics, for which a 20% Ni supported on alumina catalyst was considered, CaO hydration and undesired irreversible carbonation were also implemented in the methanator, since CO_2 was present.

Table 2. Reactions implemented in Aspen.

Reaction	Formula	ΔH_{298K} (kJ/mol)	Description
R1	$CO_2 + 4H_2 \rightleftarrows CH_4 + 2H_2O$	−165.0	CO_2 methanation
R2	$CO + 3H_2 \rightleftarrows CH_4 + H_2O$	−206.2	CO methanation
R3	$CO + H_2O \rightleftarrows CO_2 + H_2$	−41.2	Water-gas shift
R4	$CaO + H_2O \rightleftarrows Ca(OH)_2$	−65	CaO hydration
R5	$CaO + CO_2 \rightleftarrows CaCO_3$	−178	CaO carbonation

The details of the kinetic equations and their literature sources are reported in previous work by the authors [28].

In the 'REGEN' block, N_2 was fed (about 40 Nm^3/h), and $Ca(OH)_2$ was dehydrated and then fed back to the methanator. Only the reverse reaction, R4 (Table 2), was therefore implemented in this block.

Lastly, the flowsheet was completed by a 'PURGE' (Figure 2) and a fresh sorbent make-up ('SIN' in Figure 2) to avoid calcium carbonate accumulation in the loop, since the sorbent deactivated via carbonation in 'METH' cannot be regenerated through calcination in the 'REGEN' block due to the low temperature. The solid stream at the inlet of the methanator ('FEED') was fixed at 100 kg/h with the 'RECYCLE', calculated by means of the Aspen calculator block to maintain this value.

2.2. Key Parameters

The performances of the SEM process were evaluated by the definition of three different parameters that describe the compositions of the inlet gas in the methanator and the amount of the inlet flow of the sorbent CaO in relation to the gaseous reactants. The first parameter adopted in this work is α, which defines the methanation reactants feed ratio;

when $\alpha = 3$ the gas feed ratio is stoichiometric with respect to reactions R1 and R2 (Table 2), while lower values indicate a sub-stoichiometric gas feed with respect to H_2:

$$\alpha = (H_2 - CO_2)/(CO + CO_2) \tag{3}$$

where all the species are expressed in molar flows. In this work, as the biogas is simply considered as a mixture of CO_2 and CH_4, the expression of α can be simplified as follows:

$$\alpha = (H_2 - CO_2)/CO_2 \tag{3'}$$

Specifically, three different values have been investigated: $\alpha = 1,2,3$.

The parameter φ characterizes the biogas in terms of CO_2 and CH_4:

$$\varphi = CH_4/(CH_4 + CO_2) \tag{4}$$

Two specific values of φ were explored in order to simulate two opposite conditions of a biogas poor and rich in methane ($\varphi = 0.5$ and 0.7), respectively.

Lastly, the third parameter is strictly related to the SEM process, because it is a measure of the inlet sorbent amount of H_2O removal with respect to the reactant gases of the methanation process. The latter, indicated as θ, and already introduced in a previous work by the same authors [28], is defined as follows:

$$\Theta = CaO/CaO_{st} \tag{5}$$

where CaO_{st} is the stoichiometric sorbent molar flow required for the total removal of the maximum theoretical amount of H_2O that the methanation reactions can generate, considering that for each mole of steam one mole of CaO (R4) is necessary. From the R1 reaction stoichiometry, CaO_{st} is equal to $2CO_2$ if the inlet gas ratio is stoichiometric ($\alpha = 3$), or sub-stoichiometric with respect to CO_2 ($\alpha \geq 3$). Conversely, since CO is totally absent in the feeding gas with an over-stoichiometric composition with respect to CO_2 ($\alpha < 3$), the maximum amount of H_2O is linked exclusively to the quantity of H_2 as follows:

$$CaO_{st} = H_2O^{max} = H_2/2. \tag{6}$$

A complete description of the calculation of CaO_{st} in the case when both CO and CO_2 are present in the inlet gas can be found elsewhere [28].

Four distinct values of θ have been investigated: $\theta = 0$ (no SEM condition) used as a benchmark condition; $\theta = 0.5$, a sub-stoichiometric condition of CaO with respect to the quantity of steam that can be produced at most by the inlet gas in the system; $\theta = 1$, a stoichiometric condition of CaO; and $\theta = 2$ an over-stoichiometric condition of CaO.

3. Results and Discussion

3.1. SEM Performances

3.1.1. Effect of CaO on the Product Gas Quality

The effect of CaO on the product gas composition is reported in Figure 3 at different α and φ and for a fixed temperature of 300 °C. The compositions considered to be acceptable for direct injection in the grid are indicated in green, taking into account the average limits in Europe ($H_2 < 2\%$, $CO_2 < 2.5\%$, $CO < 0.5\%$ on a dry molar basis). On the other hand, the product gas compositions highlighted in red are those corresponding to operating conditions resulting in a gas quality which does not match the grid specifications.

Θ=0

φ↓	α→	3	2	1
0.5	H_2	3.9%	2.42%	1.47%
	CO_2	0.95%	12.64%	24.85%
	CO	0.035%	0.17%	0.2%
0.7	H_2	3.23%	1.89%	1.23%
	CO_2	0.77%	7.73%	14.98%
	CO	0.05%	0.14%	0.19%

Θ=0.5

φ↓	α→	3	2	1
0.5	H_2	13.49%	2.34%	1.64%
	CO_2	0%	2.39%	11.04%
	CO	0%	0.08%	0.13%
0.7	H_2	6.8%	2.04%	1.23%
	CO_2	0%	1.7%	6.45%
	CO	0%	0.09%	0.14%

Θ=1

φ↓	α→	3	2	1
0.5	H_2	27.18%	2.79%	1.84%
	CO_2	0%	0.31%	3.18%
	CO	0%	0.08%	0.12%
0.7	H_2	14.29%	1.84%	0.71%
	CO_2	0%	0.34%	0%
	CO	0%	0.07%	0.07%

Θ=2

φ↓	α→	3	2	1
0.5	H_2	47.98%	12.7%	0.94%
	CO_2	0%	0%	0%
	CO	0%	0%	0.04%
0.7	H_2	27.86%	1.85%	0.49%
	CO_2	0%	0%	0%
	CO	0%	0%	0.04%

Figure 3. H_2, CO_2, and CO molar percentages on dry basis (rest CH_4) at the outlet of methanator as a function of α, Φ, and θ at T = 300 °C. Colors: green = acceptable, red = non-acceptable (for direct grid injection).

At 300 °C, for a stoichiometric composition of the reactant gas ($\alpha = 3$), starting from the benchmark case corresponding to a traditional methanation process, where $\theta = 0$ since no CaO is fed, the outlet CO and CO_2 are lower than the maximum concentrations accepted. The critical value, as also reported in the literature from purely thermodynamic considerations [24], is the H_2 at the outlet, which is above 2% for both the φ considered. The dependence of the outlet gas concentration on φ is quite low. The H_2 concentration slightly approaches the grid standard with φ increasing from 0.5 to 0.7. Although the H_2 conversion decreases in the case of an inlet feeding gas richer in CH_4 ($\varphi = 0.7$) as expected, the lower H_2 concentration under this case is due to the better inlet gas quality in terms of methane and the lower stoichiometric H_2 amount required for CO_2 methanation. Overall, no condition fulfills the required specifications for a stoichiometric ($\alpha = 3$) feed at 300 °C. Under a sub-stoichiometric ratio when $\alpha = 2$, an overturning of the product gas behavior occurs compared to the $\alpha = 3$ case. When $\alpha = 2$, the CO_2 outlet composition now does not match the standards. This concentration strongly increases with respect to the stoichiometric feed, moving from less than 1% to 12.64% and 7.73% for $\varphi = 0.5$ and $\varphi = 0.7$, respectively. On the contrary, the H_2 output decreases at $\alpha = 2$, as expected, but is more weakly affected by α than CO_2. In particular, if considering the value of H_2 corresponding to the $\varphi = 0.7$ case, it would respect the limit concentration for injection under this sub-stoichiometric condition. CO also increases compared to the $\alpha = 3$ condition, but its concentration is still much lower than the limit. However, once again, no condition can be detected for the direct injection into the grid. The same conclusion can be drawn for $\alpha = 1$, where the CO_2 concentrations are higher than in the previous case; with the lowest H_2 amount fed to the system ($\alpha = 1$), its concentration also fulfills the limit for $\varphi = 0.5$, unlike the $\alpha = 2$ case where only at $\varphi = 0.7$ was its concentration below 2%. Although CO increases as α decreases, this species still remains below the limit.

When considering the results of the actual SEM process, with a sub-stoichiometric CaO injection in the reactive system ($\theta = 0.5$), and for the stoichiometric gas feed case ($\alpha = 3$), the H_2 outlet dramatically increases with respect to the benchmark case and a detrimental

effect of the CaO can thus be identified. In particular, the undesired CaO carbonation reaction results in a removal of CO_2, subtracting it from the methanation reaction and accelerating the consumption of CO in the WGS reaction, implying the production of more H_2. Indeed, unlike the $\theta = 0$ case, no carbon-containing contaminants are detected at the outlet. When considering sub-stoichiometric feed with respect to H_2 ($\alpha = 2$), the presence of CaO keeps the CO_2 at the outlet below the limit unlike the traditional methanation case ($\theta = 0$). However, under this condition the H_2 amount is still above the limit for the two φ considered. For $\alpha = 1$, the outlet condition is reversed: the decreased H_2 feeding involves a sufficient decrease in H_2 at the outlet for injection in the grid, but the effect of CaO cannot counteract the strong increase in CO_2 for such a H_2-lean feeding. The CO contaminant slightly increases at the outlet with α decreasing, similarly to what happens for the $\theta = 0$ case. Again, under $\theta = 0.5$ conditions, no gas outlet matches the grid specifications. However, given the reversal behavior between H_2 and CO_2 moving from $\alpha = 2$ to $\alpha = 1$, it could be possible that for an intermediate value of α both species meet grid restrictions. When considering stoichiometric CaO feeding ($\theta = 1$), the same trend observed with $\theta = 0.5$ can be summarized. For a stoichiometric gas feed ($\alpha = 3$), the composition in terms of H_2 clearly worsens by increasing the sorbent feed; however, for the sub-stoichiometric value of $\alpha = 2$, an optimal working condition can be identified for the direct injection into the grid corresponding to the $\varphi = 0.7$ case. Lastly, for the over-stoichiometric CaO fed to the system ($\theta = 2$) and for the lowest alfa considered (alfa = 1), the excess of CO_2 is also offset by carbonation for $\varphi = 0.5$. Under these working conditions, the contaminants at the outlet meet the grid specifications.

3.1.2. Effect of Temperature on the Product Gas Quality

Regarding the methanation temperature effect, when the temperature is increased, thermodynamic conditions become more unfavorable and, predictably, the performance becomes worse (Figure 4).

$\Theta=0$					$\Theta=0.5$			
$\phi\downarrow$ $\alpha\rightarrow$		3	2	1	$\phi\downarrow$ $\alpha\rightarrow$	3	2	1
	H_2	10.95%	7.16%	5.69%	H_2	21%	13%	7.24%
0.5	CO_2	2.48%	12.95%	24.23%	0.5 CO_2	0%	1.3%	7.24%
	CO	0.34%	0.59%	1.03%	CO	0%	0.3%	0.6%
	H_2	10.86%	6.45%	4.62%	H_2	12%	12%	7.85%
0.7	CO_2	2.45%	8.16%	14.69%	0.7 CO_2	0.03%	1.09%	4.45%
	CO	0.33%	0.61%	1.04%	CO	0.03%	0.6%	1.26%

$\Theta=1$					$\Theta=2$			
$\phi\downarrow$ $\alpha\rightarrow$		3	2	1	$\phi\downarrow$ $\alpha\rightarrow$	3	2	1
	H_2	38.72%	10.51%	7.27%	H_2	55%	27.27%	4.82%
0.5	CO_2	0%	0.21%	0.69%	0.5 CO_2	0%	0%	0%
	CO	0%	0.18%	0.31%	CO	0%	0%	0%
	H_2	21%	6.92%	4.67%	H_2	35%	13%	4.1%
0.7	CO_2	0%	0.03%	0.56%	0.7 CO_2	0%	0%	0%
	CO	0%	0.06%	0.2%	CO	0%	0.06%	0.09%

Figure 4. H_2, CO_2, and CO molar percentages on dry basis (rest CH_4) at the outlet of methanator as a function of α, Φ, and θ at T = 350 °C. Colors: green = acceptable, red = non-acceptable (for direct grid injection).

By increasing the temperature from 300 to 350 °C, under traditional methanation conditions ($\theta = 0$) and $\alpha = 3$, the outlet CO_2 for both φ is only slightly below the limit value for the injection, demonstrating a worsened performance compared to 300 °C. Indeed, unlike the 300 °C case, the H_2 concentration remains above the limit even when considering sub-stoichiometric feeds (7.16% and 5.69% for $\alpha = 2$ and $\alpha = 1$, respectively).

As for the SEM process with different CaO amounts fed to the methanator (θ varying from 0.5 to 2), results may be summarized as follows:

- CO, which is not a reactant in this biogas upgrading scheme but can be formed by other reaction paths such as the Reverse Water Gas Shift reaction, increases with α decreasing and tends to decrease for the highest values of θ. However, it is always below the limit;

- CO_2 is always below the limit except for when the sub-stoichiometric value of CaO ($\theta = 0.5$) and $\alpha = 1$; under this condition the sorbent fed is still not sufficient to compensate CO_2 excess in the feed gas;

- H_2 represents, again, the critical species, always being above the limit value even for the best conditions in terms of its consumption, and namely under the limit case with minimum α and maximum θ, where the H_2 detected is about 4% for both values of φ.

Overall, at 350 °C no parameter values can be identified as optimal working conditions for the direct injection of the product gas.

At the lowest temperature investigated (250 °C), the process is clearly thermodynamically favored (Figure 5). For a stoichiometric feed and conventional methanation, the product stream is already injectable in the grid.

Θ=0		3	2	1
φ↓	α→	3	2	1
0.5	H_2	1.33%	0.32%	0.32%
	CO_2	0.33%	12.47%	24.93%
	CO	0%	0%	0.04%
0.7	H_2	1.14%	0.46%	0.34%
	CO_2	0.28%	7.47%	14.96%
	CO	0%	0.03%	0.03%

Θ=0.5		3	2	1
φ↓	α→	3	2	1
0.5	H_2	5.96%	0.52%	0.33%
	CO_2	0%	5.64%	14.25%
	CO	0%	0%	0%
0.7	H_2	3.04%	0.42%	0.28%
	CO_2	0%	3.53%	9.07%
	CO	0%	0.03%	0.05%

Θ=1		3	2	1
φ↓	α→	3	2	1
0.5	H_2	14.56%	0.35%	0.3%
	CO_2	0%	2.17%	8.79%
	CO	0%	0%	0.05%
0.7	H_2	6.97%	0.3%	0.24%
	CO_2	0%	1.5%	5.39%
	CO	0%	0.04%	0.05%

Θ=2		3	2	1
φ↓	α→	3	2	1
0.5	H_2	29.68%	0.05%	0%
	CO_2	0%	0%	0.15%
	CO	0%	0.05%	0%
0.7	H_2	13.9%	0%	0%
	CO_2	0%	0%	0.13%
	CO	0%	0.04%	0.2%

Figure 5. H_2, CO_2, and CO molar percentages on dry basis (rest CH_4) at the outlet of methanator as a function of α, Φ, and θ at T = 250 °C. Colors: green = acceptable, red = non-acceptable (for direct grid injection).

However, when considering an α decrease, i.e., the realistic conditions for an industrial process at sub-stoichiometric feed in terms of H_2, an increase in CO_2 occurs, as was also the case at 300 °C and 350 °C. Again, the molar CO_2 percentage is around 13% and 25% at $\varphi = 0.5$ and 8%, and 15% at $\varphi = 0.7$ for α equal to 2 and 1, respectively. The values

under these conditions are similar for all the temperatures considered. Unlike traditional methanation, no conditions ensure a directly injectable outlet gas when considering $\alpha = 3$ with the introduction of CaO due to the negative outcome on the outlet H_2 amount. As for $\alpha < 3$, the H_2 composition is always suitable for injection even at $\theta = 0.5$, while for this sub-stoichiometric value of CaO feed, the CO_2 percentage is still above the limit. At $\alpha = 2$, since the CO_2 amount remarkably decreases with θ, working conditions acceptable in terms of contaminants can be found from the stoichiometric value of CaO ($\theta = 1$) onward. Lastly, for $\theta = 2$, an optimal condition is also detected for $\alpha = 1$.

3.2. SEM Thermodynamics and Possible Carbon Formation

Ternary diagrams C-H-O have been used to detect possible thermodynamic conditions for carbon generation for the system under scrutiny. Figure 6 reports in triangular coordinates the molar fraction of C-H-O elements in the gas phase and the calculated carbon formation boundaries for the different temperatures [24]. The points constituting the isotherms (green, blue, and red dashed lines in Figure 6) are the combinations of values for C-H-O elements in the gas phase in equilibrium with solid carbon. Above the lines coke deposition is possible from a thermodynamic point of view. The dots in the ternary diagram indicate the different feeding gas ratios.
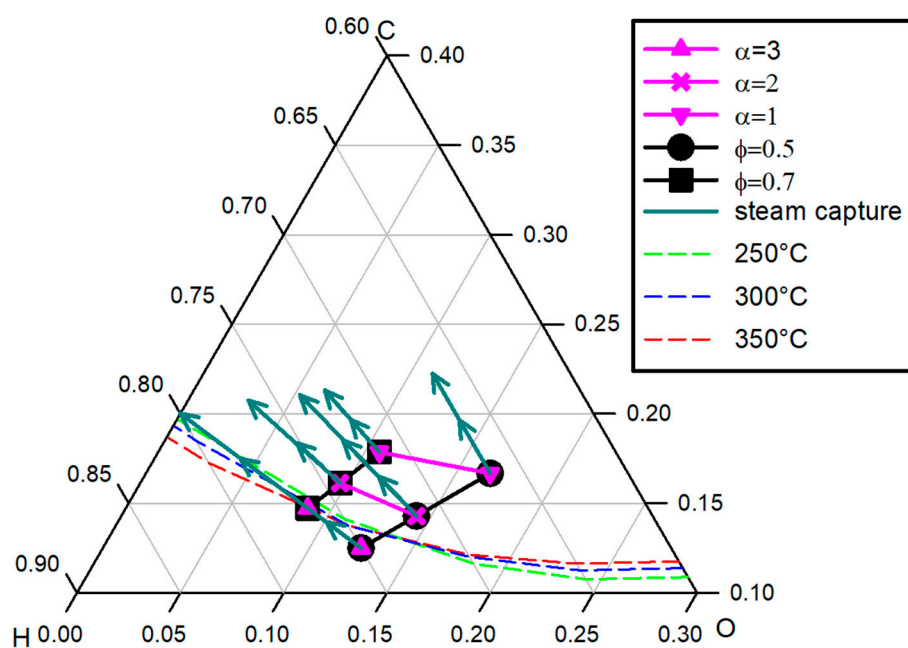
Figure 6. C-H-O ternary diagram reporting carbon deposition boundaries (at $p = 1$ atm and temperatures in the range 250–350 °C) and the feed compositions at different values of α and Φ. The straight lines reproduce the reaction environment composition after progressive steam removal.

Evidently, with conventional methanation ($\theta = 0$), the feeding gas and the outlet compositions coincide in terms of C-H-O molar fractions. On the other hand, H_2O removal from the system (SEM conditions) makes the feeding points move toward the upper zone of the graph, leading to an enrichment of C in the system as indicated by the straight lines in Figure 6 ('steam capture' lines). The complete removal of steam from the reaction environment in the 'stoichiometric case' ($\alpha = 3$) would determine pure CH_4 as the outlet composition point (on the H-C axis). Differently, for $\alpha < 3$, the final value would correspond to a mixture also containing oxygen due to the excess carbon oxide compounds (CO and CO_2). Moreover, it can be noted that 'stoichiometric' feeding dots ($\alpha = 3$) fall outside the carbon generation area, in particular, when φ is equal to 0.5. When the feeding is characterized by $\varphi = 0.7$, it falls just on the boundary line of carbon formation at 350 °C (red line in Figure 6). On the contrary, all feeding gases with $\alpha < 3$ are located within the

carbon deposition area. Under these conditions, even if considering traditional (no-SEM) methanation, carbon generation is favored from a thermodynamic point of view. For all the locations of the feeding dots (inside or outside the carbon formation zone), looking at Figure 6 it is clear that the capture of only steam always leads to the region favored for carbon formation. However, the situation is more complicated using CaO as a sorbent due to its ability to react with both H_2O and CO_2. In this last case, a subtraction of C will occur besides H and O and the 'migration paths' of feeding dots would be different from the conditions under which only H_2O is removed. These paths would depend on the amount of sorbent θ, its different intrinsic affinity with CO_2 and H_2O, and how the temperature influences the kinetics of the reactions. In Figure 7 the C-H-O migration paths at different values of θ and different methanation temperature are reported for one selected condition of α and φ.
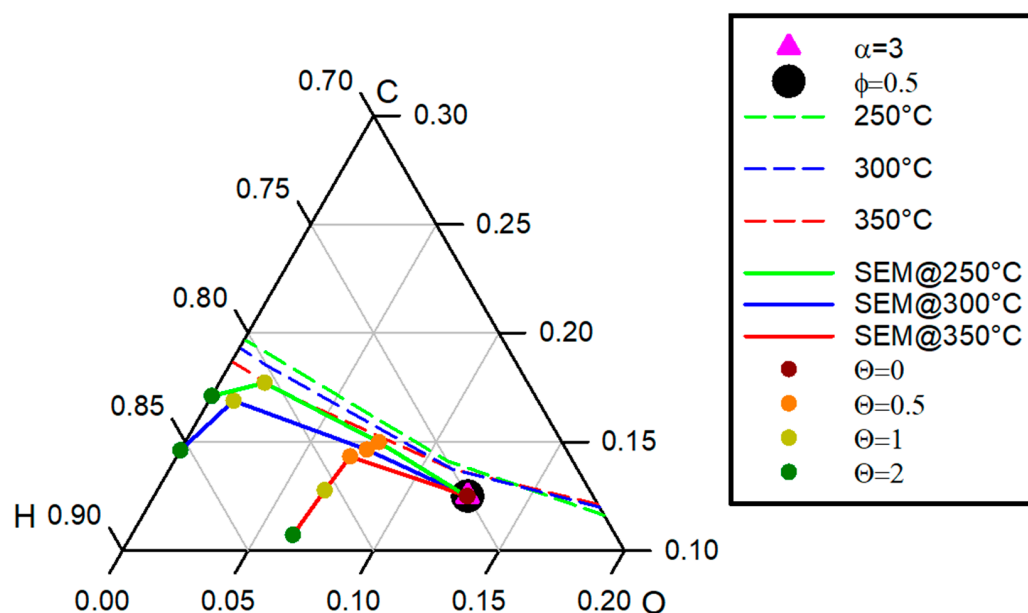
Figure 7. C-H-O ternary diagram with computed C-H-O points from SEM simulations with CaO (α = 3, Φ = 0.5, and for different values of θ).

CaO SEM curves tend to achieve compositions richer in H and C, since a significant consumption of O occurs under these conditions. The higher the temperature, the more the migration paths move away from those relative to only steam removal since higher temperatures favor higher CO_2 capture. Regarding the temperature range of this work, the C deposition is likely to be quite slow [29], especially when considering the effective temperature control of a fluidized bed configuration. In addition, the combined CO_2 and H_2O removal keeps the system closer to the boundaries of the carbon deposition area, which could be a further benefit for reducing the carbon generation. However, since CaO, $Ca(OH)_2$, and $CaCO_3$ could also affect the carbon generation kinetics, further experiments should confirm these predictions.

4. Conclusions

Biogas upgrading by SEM in DIFB considering CaO as sorbent was simulated in ASPENplus, with the aim of analyzing the worsening effect of the parallel carbonation reaction and detecting possible working conditions to reach suitable product gas, in terms of contaminants, for direct injection it into the natural gas grid. The simulations involved the study of the effect of the feed composition (in terms of α and φ) and CaO fed to the system (θ), as well as the effect of the methanation temperature in the range 250–350 °C.

A traditional methanation process would entail the possible direct injection exclusively for the lowest methanation temperature of 250 °C and only for a stoichiometric gas feeding

(α = 3). However, it may be worth underlining that a 250 °C operating temperature is more of a theoretical limit, while the catalyst would be sufficiently active only from higher temperatures.

As for the SEM process, the extent of the detrimental effect of CaO carbonation, resulting in increasing H_2 concentration, determines that with stoichiometric gas (α = 3) no conditions can fulfill the grid specifications even at the lowest temperature of 250 °C. As for sub-stoichiometric conditions, with respect to H_2 ($\alpha < 3$), the outlet gas quality improves by increasing CaO, with the CO_2 excess being compensated by CaO carbonation. The detected gas and CaO feedings able to produce a suitable gas for injection can be summarized as a function of the process temperature. For example, at 300 °C for α = 2 and φ = 0.7 (CH_4-rich biogas), the produced gas composition is suitable for the gas grid from a stoichiometric value of CaO (θ = 1) onward, while if considering φ = 0.5 (CH_4-lean biogas), this is true only for α = 1 and an over-stoichiometric value of CaO (θ = 2). At 250 °C, a suitable gas is obtained for both biogas compositions considered: for α = 2 from θ = 1 onward, and for α =1 at θ =2. On the contrary, for the higher methanation temperature of 350 °C, no conditions are detected for a proper outlet gas quality.

In conclusion, as long as a sub-stoichiometric gas with respect to H_2 is fed to the process, it is possible to select CaO as a possible sorbent material to carry out SEM. In the framework of the power-to-methane processes, H_2-lean feedings are of interest considering the wide range of possible conditions and flexibility required to manage the fluctuations associated with such applications. Since a thermodynamic study indicated that with H_2O capture carbon formation cannot be excluded, especially under sub-stoichiometric H_2 feed, an experimental study may be required to identify the actual extent of carbon deposition under such conditions.

Author Contributions: Conceptualization, F.S. and A.C.; methodology, F.M., F.S. and A.C.; software, F.M. and A.C.; validation, F.M. and A.C.; formal analysis, F.M. and A.C.; investigation, A.C. and F.S.; data curation, F.M. and A.C.; writing—original draft preparation, F.S. and A.C.; writing—review and editing, F.M., F.S. and A.C. All authors have read and agreed to the published version of the manuscript.

Data Availability Statement: Data available on request.

References

1. Götz, M.; Lefebvre, J.; Mörs, F.; McDaniel Koch, A.; Graf, F.; Bajohr, S.; Reimert, R.; Kolb, T. Renewable Power-to-Gas: A technological and economic review. *Renew. Energy* **2016**, *85*, 1371–1390. [CrossRef]
2. Rönsch, S.; Schneider, J.; Matthischke, S.; Schlüter, M.; Götz, M.; Lefebvre, J.; Prabhakaran, P.; Bajohr, S. Review on methanation—From fundamentals to current projects. *Fuel* **2016**, *166*, 276–296. [CrossRef]
3. Koytsoumpa, E.I.; Karellas, S. Equilibrium and kinetic aspects for catalytic methanation focusing on CO_2 derived Substitute Natural Gas (SNG). *Renew. Sustain. Energy Rev.* **2018**, *94*, 536–550. [CrossRef]
4. Farghali, M.; Osman, A.I.; Umetsu, K.; Rooney, D.W. Integration of biogas systems into a carbon zero and hydrogen economy: A review. *Environ. Chem. Lett.* **2022**, *20*, 2853–2927. [CrossRef]
5. Tawfik, A.; Mohsen, M.; Ismail, S.; Alhajeri, N.S.; Osman, A.I.; Rooney, D.W. Methods to alleviate the inhibition of sludge anaerobic digestion by emerging contaminants: A review. *Environ. Chem. Lett.* **2022**, *20*, 3811–3836. [CrossRef]
6. Faria, A.C.; Miguel, C.; Madeira, L.M. Thermodynamic analysis of the CO_2 methanation reaction with in situ water removal for biogas upgrading. *J. CO_2 Util.* **2018**, *26*, 271–280. [CrossRef]
7. Sabatier, P. New synthesis of methane. *Comptes Rendus* **1902**, *134*, 514–516.
8. HaldorTopsoe. *From Solid Fuels to Substitute Natural Gas (SNG) Using TREMP*; Technical Report; Haldor Topsoe: Lyngby, Denmark, 2009.
9. Duyar, M.S.; Treviño, M.A.A.; Farrauto, R.J. Dual function materials for CO_2 capture and conversion using renewable H_2. *Appl. Catal. B Environ.* **2015**, *168–169*, 370–376. [CrossRef]
10. Mills, G.A.; Steffgen, F.W. Catalytic Methanation. *Catal. Rev.* **1974**, *8*, 159–210. [CrossRef]
11. Bartholomew, C.H. Mechanisms of catalyst deactivation. *Appl. Catal. A Gen.* **2001**, *212*, 17–60. [CrossRef]

12. Walspurger, S.; Elzinga, G.D.; Dijkstra, J.W.; Sarić, M.; Haije, W.G. Sorption enhanced methanation for substitute natural gas production: Experimental results and thermodynamic considerations. *Chem. Eng. J.* **2014**, *242*, 379–386. [CrossRef]
13. Borgschulte, A.; Gallandat, N.; Probst, B.; Suter, R.; Callini, E.; Ferri, D.; Arroyo, Y.; Erni, R.; Geerlings, H.; Züttel, A. Sorption enhanced CO_2 methanation. *Phys. Chem. Chem. Phys.* **2013**, *15*, 9620–9625. [CrossRef] [PubMed]
14. Delmelle, R.; Duarte, R.; Franken, T.; Burnat, D.; Holzer, L.; Borgschulte, A.; Heel, A. Development of improved nickel catalysts for sorption enhanced CO_2 methanation. *Int. J. Hydrogen Energy* **2016**, *41*, 20185–20191. [CrossRef]
15. Dou, B.; Zhang, H.; Cui, G.; Wang, Z.; Jiang, B.; Wang, K.; Chen, H.; Xu, Y. Hydrogen production and reduction of Ni-based oxygen carriers during chemical looping steam reforming of ethanol in a fixed-bed reactor. *Int. J. Hydrogen Energy* **2017**, *42*, 26217–26230. [CrossRef]
16. Dou, B.; Zhang, H.; Cui, G.; Wang, Z.; Jiang, B.; Wang, K.; Chen, H.; Xu, Y. Hydrogen production by sorption-enhanced chemical looping steam reforming of ethanol in an alternating fixed-bed reactor: Sorbent to catalyst ratio dependencies. *Energy Convers. Manag.* **2018**, *155*, 243–252. [CrossRef]
17. Müller, S.; Fuchs, J.; Schmid, J.; Benedikt, F.; Hofbauer, H. Experimental development of sorption enhanced reforming by the use of an advanced gasification test plant. *Int. J. Hydrogen Energy* **2017**, *42*, 29694–29707. [CrossRef]
18. Coppola, A.; Massa, F.; Salatino, P.; Scala, F. Evaluation of two sorbents for the sorption-enhanced methanation in a dual fluidized bed system. *Biomass-Convers. Biorefin.* **2020**, *11*, 111–119. [CrossRef]
19. Agirre, I.; Acha, E.; Cambra, J.; Barrio, V. Water sorption enhanced CO_2 methanation process: Optimization of reaction conditions and study of various sorbents. *Chem. Eng. Sci.* **2021**, *237*, 116546. [CrossRef]
20. Seemann, M.; Schildhauer, T.; Biollaz, S.; Stucki, S.; Wokaun, A. The regenerative effect of catalyst fluidization under methanation conditions. *Appl. Catal. A Gen.* **2006**, *313*, 14–21. [CrossRef]
21. Gao, J.; Wang, Y.; Ping, Y.; Hu, D.; Xu, G.; Gu, F.; Su, F. A thermodynamic analysis of methanation reactions of carbon oxides for the production of synthetic natural gas. *RSC Adv.* **2012**, *2*, 2358. [CrossRef]
22. Frick, V.; Brellochs, J.; Specht, M. Application of ternary diagrams in the design of methanation systems. *Fuel Process. Technol.* **2014**, *118*, 156–160. [CrossRef]
23. Swapnesh, A.; Srivastava, V.C.; Mall, I.D. Comparative study on thermodynamic analysis of CO_2 utilization reactions. *Chem. Eng. Technol.* **2014**, *37*, 1765–1777. [CrossRef]
24. Massa, F.; Coppola, A.; Scala, F. A thermodynamic study of sorption-enhanced CO_2 methanation at low pressure. *J. CO_2 Util.* **2019**, *35*, 176–184. [CrossRef]
25. Werther, J. Fluidized-bed reactors. In *Ullmann's Encyclopedia of Industrial Chemistry*; Wiley: Hoboken, NJ, USA, 2007; ISBN 9783527303854. [CrossRef]
26. Kunii, D.; Levenspiel, O. *Fluidization Engineering*; Butterworth-Heinemann: Boston, MA, USA, 1991.
27. Yang, W. *Handbook of Fluidization and Fluid-Particle Systems*; CRC Press: Boca Raton, FL, USA, 2003.
28. Coppola, A.; Massa, F.; Scala, F. Simulation of a sorption-enhanced methanation process with CaO in a dual interconnected fluidized bed system. *Fuel* **2023**, *339*, 127374. [CrossRef]
29. Gardner, D.C.; Bartholomew, C.H. Kinetics of Carbon Deposition During Methanation of CO. *Ind. Eng. Chem. Prod. Res. Dev.* **1981**, *20*, 80–87. [CrossRef]